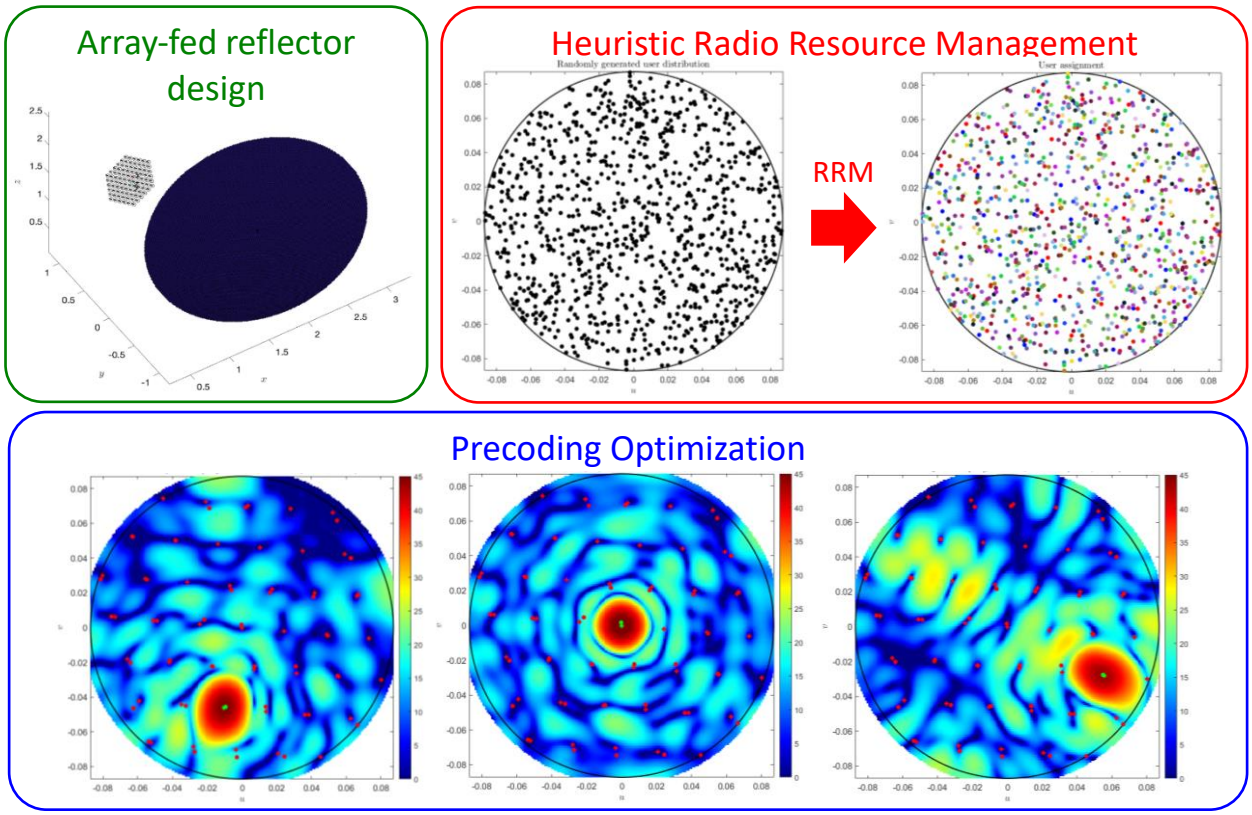

Pragmatic design and monitoring of array-fed reflector payload

Executive Summary Report
co-sponsored research

OSIP Channel: (v1) Early Technology Development

Affiliation(s): Heriot-Watt University (Prime), Thales Alenia Space France (Subcontractor)

Activity summary:
In the framework of this project, we propose an innovative pragmatic and reconfigurable array-fed reflector payload for broadband missions in Ku band for GEO missions. First, the antenna sub-system was optimized through physical optics-based simulations obtained with an in-house simulation tool written in Matlab. A fixed-beam beamforming network architecture was proposed to limit the complexity of the system. Combined with an updated version of the heuristic radio resource management algorithm, the system achieved satisfactory performance with limited complexity. The final architecture's performance has been validated through numerical simulation in both uniform and non-uniform traffic scenarios.

Publishing Date: 23 August 2024
Contract Number: 4000138743/22/NL/GLC/ov
Implemented as ESA Initial Support for Innovation

1 Introduction and Motivation

The present document corresponds to the executive summary report of the OSIP project titled "Pragmatic design and monitoring of array-fed reflector payloads" funded by the European Space Agency under contract No. 4000138743/22/NL/GLC/ov. The three partners involved in the project are Heriot-Watt University (Edinburgh, UK), Thales Alenia Space (Toulouse, France), and the European Space Agency (Noordwijk, Netherlands).

The main project's goal consisted in the development of a pragmatic array-fed reflector (AFR) architecture for a multi-beam broadband communication satellite in geostationary orbit (GEO). While single-feed-per-beam (SFPB) architectures have dominated the market in the last decade, the industry is moving towards reconfigurable architectures, equipped with a digital transparent processor (DTP) connected to an array of active antennas [1]. Reconfigurable payloads allow to adapt the available resources, such as frequency allocation and power per beam, to the current traffic scenario in order to maximise the total throughput of the satellite. In addition, this solution supports both broadcast (same signal transmitted over a wide region) and broadband (cellular like coverage with different signals transmitted to different users with narrow beams) missions. In fact, the DTP allows to digitally generate multiple spot beams within a coverage region or synthesize a broad beam that covers all the target region. Consequently, the same payload could serve for a broadcast mission and then transition to a broadband one, with joint broadband and broadcast transmission during the transition phase. Finally, since the satellite can be reconfigured electronically, a single antenna design could be used for every coverage, drastically reducing the cost per unit.

AFRs provide an optimal trade-off for GEO satellites: the presence of a large parabolic reflector allows to reduce the feed array size compared to a direct radiating architecture (DRA) without penalizing the gain. Consequently, the number of radiating elements can be reduced accordingly, and each element connected to one of the input/output ports of the DTP. In fact, the number of I/O ports supported by a state-of-the-art DTP does not exceed a few hundreds [2], which is a small value compared to the number of radiating elements in a GEO DRA architecture. The main drawback of a parabolic AFR architecture is its uneven distribution of the power across the feed array, that could result in an underuse of the available output power of the amplifiers of each active antenna. However, a better distribution of the power can be achieved by shaping the reflector, i.e. moving from a parabolic shape to a perturbation of a parabolic shape. On the other hand, the shaping results in a penalisation of the directivity.

Despite the clear benefits, reconfigurability comes at a price: an increased computational effort is demanded to the DTP to compute the precoding matrix and to perform radio resource management (RRM). In [3], the authors proposed a pragmatic solution that allows to significantly reduce the computational cost in a DRA architecture. The key idea is to avoid the precoding matrix computation by adopting an architecture consisting in a fixed-beam beamforming network (FB-BFN) followed by a beam-selection matrix. Furthermore, the FB-BFN network can be efficiently implemented using the FFT algorithm in a DRA architecture. In the framework, of the project we developed a similar architecture with a FB-BFN. However, due to the different propagation channel, in an AFR this cannot

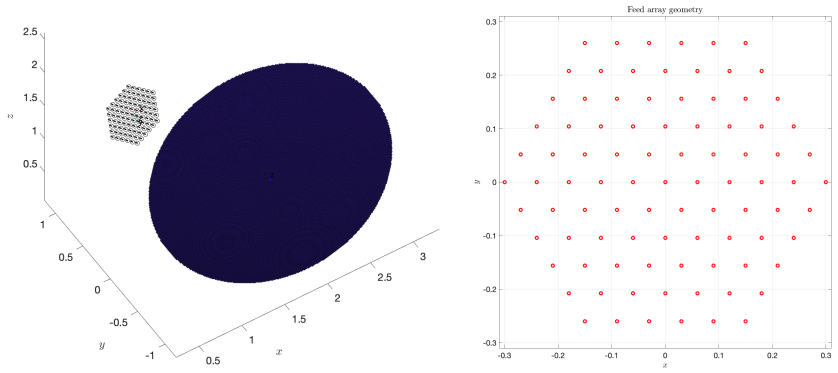

(a) (b)

Figure 1: (a) 3D view of the AFR system; (b) Feed array element position.

implemented using the FFT algorithm. Consequently, the proposed architecture consists in computing the FB-BFN weights on a regular grid of points in the u-v plane, which are then stored on the satellite. Since the computation of the beamforming weights can be done on Earth, minimum mean square error (MMSE) precoding can be applied to generate beams with nulls placed at the other beams' location. Once computed, the beamforming weights are transmitted to the satellite through the feeder link.

Considering the RRM problem, its complexity does not allow to find an optimal solution when a large number of users is considered. Consequently, an heuristic RRM (H-RRM) algorithm is described in [4] that minimizes the total interference and guarantees performance close to optimal, but with linear complexity. However, the algorithm is developed for time division multiplexing (TDM) systems with perfectly orthogonal time slots. In the framework of the project, the algorithm was extended to any type of system multiplexing scheme, such as frequency (FDM) or code (CDM) division multiplexing. Furthermore, the new version of the algorithm allows to maximize the SNIR, instead of minimizing the interference, which results in a significant improvement of the performance.

2 Use Case Definition

In the framework of the project, we considered a Ku user downlink use case (from 10.70GHz to 12.75GHz). The available band is split in 41 bands of 50MHz each. Fig.1 shows the AFR system. The reflector has a diameter of 2.4m, while the array consists in 91 elements arranged on an hexagonal lattice with inter-element spacing equal to 0.06m. Each radiating element is simulated as a vertically-polarized ideal gaussian source.

The system is optimized for two different coverages: one continental coverage, represented in Fig.2a and corresponding to a circle with radius 5°, and one regional coverage, represented in Fig.2b and corresponding to an ellipse with 3° and 4° as its minor and major semi-axis, respectively. A uniform distribution of users, arranged on an hexagonal lattice, is considered for the reflector optimization, as shown in Fig.2. The choice of optimizing the

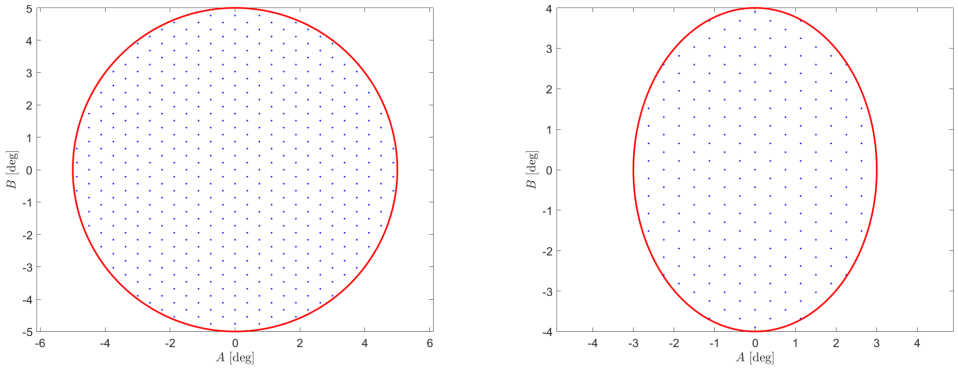

(a) Continental. (b) Regional.

Figure 2: Continental and regional coverage expressed in (A, B) coordinates.

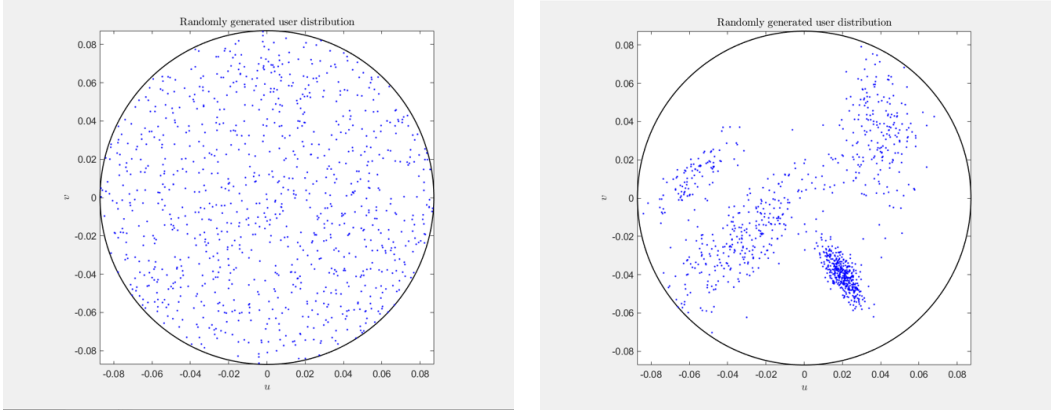

(a) Uniform. (b) Non uniform.

Figure 3: Plot of a randomly generated population with 1000 users. (a) Uniform distribution; (b) Non uniform distribution.

system for such simple coverages and considering a uniform distribution of users is in line with the project's objective: finding a common architecture that can fit different traffic scenarios.

To assess the final performance of the system, randomly generated user populations are considered. Fig.3a shows a randomly generated population of 1000 users within the continental coverage. The population is generated according to a uniform distribution. On the other hand, Fig.3b shows a population of 1000 users generated using a highly non-uniform probability density function. Populations with different numbers of users have been considered when evaluating the performance of the system.

3 Modelling Tool Development

The first project's activity consisted in the development of a modelling tool that allows to evaluate the performance of the system considering both the electromagnetic (EM) simulation and the processing. The developed code resulted in an extended version of the HERAS tool [5]. The original version of the tool was a physical optics-based EM solver for reflectors entirely written in Matlab object oriented. The following are the main modifications that have been introduced in the tool:

- Support of feed arrays.
- Support of Zernike polynomials-based shaped reflector.
- Support of geometrical optics-based aperture distribution method (GO-AD) with FFT implementation.
- Support of GPU acceleration for both the physical optics-based current distribution (PO-CD) and GO-AD methods.
- Support of lattices for the generation of the array geometry and regular coverages.
- Support of both deterministic and randomly generated traffic distributions.
- Line-of-sight channel modelling.
- Support of several precoding techniques.
- Support of RRM algorithms.
- Support of performance evaluation classes.

4 Antenna System Optimization

In this section we briefly describe the optimization algorithm that has been developed for the design of the shaped AFR. In particular, the objective was to optimize a single shaped reflector in two configurations, each corresponding to a different defocusing of the feed array (to be optimised), that maximise the performance over the two coverages described in the previous section. The objectives to be optimized are the average directivity of the beams centered on the regular lattices in Fig.2 and the power amplifier dynamics, i.e. the distribution of the power across the radiating elements when all the signals are

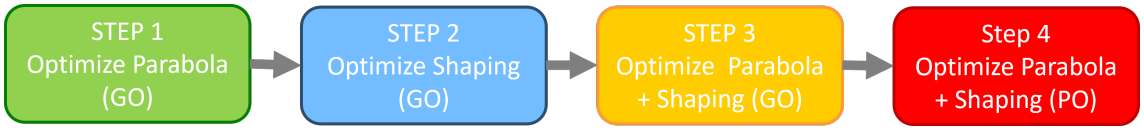

Figure 4: Shaped Array-fed reflector optimization algorithm flow graph.

Metric	Continental Coverage		Regional Coverage	
	Shaped reflector (TAS)	Shaped reflector (HWU)	Shaped reflector (TAS)	Shaped reflector (HWU)
$G_{c,\text{avg}}$ (dBi)	44.51	44.51	44.67	44.64
η_{P2P} (dB)	1.29	1.19	3.08	2.52

Table 1: Performance comparison between the optimized shaped reflector provided by TAS and the one obtained with the proposed optimization algorithm. $G_{c,\text{avg}}$: average gain. η_{P2P} peak-to-peak input power dynamic.

combined. To validate the performance, an extensive comparison has been carried out with the architecture optimised by Thales Alenia Space engineers using a completely different optimization algorithm.

To model the shaped reflector, we considered a parabolic reflector that is perturbed by adding a superposition of a set of functions (basis functions). Specifically, Zernike polynomials have been identified as the set of basis functions [6]. Zernike polynomials are a set of entire domain functions defined within the unit circle that have been extensively used in the field of optics.

Fig.4 shows the flow graph of the multi-stage optimization algorithm that has been developed. The first step consists in the optimization of the parabolic reflector parameters based on simple ray tracing considerations and general purpose optimization algorithms available in Matlab. Since the number of optimization variables is very limited, this step is extremely fast to compute. The shaping optimization follows in the second step. Here, the parabolic surface parameters are fixed and only the shaping is optimised. The optimisation algorithm is a multi-objective optimisation algorithm described in [7] that had to be coded in Matlab. In this step, the GO-AD method described in [8] is applied to perform the EM simulation. This allows to significantly reduce the simulation time compared to the more accurate PO-CD method. This is a critical aspect, since the multi-objective optimization algorithm requires hundreds or even thousands of evaluations of the objectives, and each corresponds to a full EM simulation. Consequently, reducing the EM simulation time was critical in making the optimization possible. Finally, the third and fourth step consists in a refinement of the solution, where both the parabola and the shaping are optimised using the GO-AD and PO-CD based multi-objective algorithms, respectively. However, the results suggest that these two steps can be removed at the expense of a small penalisation of the performance.

Table.1 shows the performance comparison of the shaped reflector optimised by Thales Alenia Space (TAS) engineers and the one optimised with the proposed algorithm at Heriot-Watt University (HWU). Despite the comparable average gain values, the HWU reflector achieves better performance in terms of power distribution across the array in both configurations. In addition, the total optimization took half an hour on a server at Heriot-Watt University with 24GB of dedicated GPU memory. This result was achieved because of the GPU accelerated GO-AD method in combination with a limited number of optimization variables required using Zernike's polynomial.

5 Fixed-beam Beamforming Matrix

To simplify the payload architecture, the digital beamforming network (DBFN) is realized by the cascade of a beam selection matrix, which associates each user to the beam with the closest beam centre, and a FB-BFN. The FB-BFN corresponds to a precomputed set of beamforming weights that are stored in memory. Each colour corresponds to a grid of beams arranged on a regular lattice. Fig.5 shows each colour's grid beam centres. The grids are obtained using lattice theory. In particular, we developed an algorithm that numerically finds the sub-lattice of a given lattice with an arbitrary number of colours that maximises the distance with the closest same-colour neighbour. The algorithm is extremely efficient since it exploits fundamental results in number theory to avoid the evaluation of equivalent solutions. Consequently, each colour's grid corresponds to a translated version of the same grid. This guarantees a uniform coverage while minimising the interference.

Since the FB-BFN beamforming weights associated to all the beams are computed on Earth and transmitted to the satellite through the feeder link, MMSE precoding can be applied, instead of the simpler matched filter (MF) precoding. This leads to a significant improvement of the system performance because each beam's centre corresponds to a null of all the remaining beams in the same colour. For example, Fig.6 shows three beams in colour 1. The green cross represents the corresponding beam centre, while the red crosses the remaining beams' centre in the same colour grid. From the three plots it can be observed that each beam produces nulls at the other beams' location. The nulls are not perfect for the following reason: the deeper the nulls the larger the deterioration of the main beam's gain, consequently there is no advantage in creating very deep nulls since the

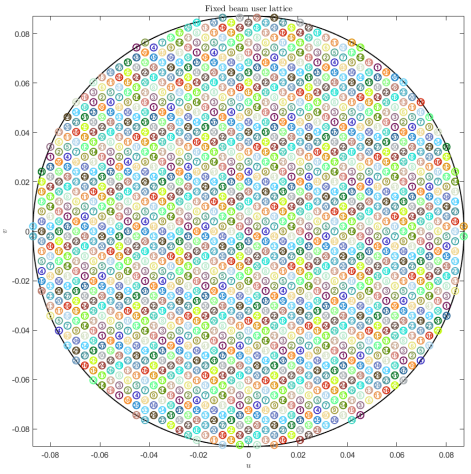

Figure 5: Plot of the beam centre's location of all the beams in all colours. Each colour's grid corresponds to a sub-lattice with 41 colours of an hexagonal lattice. The selected sub-lattice maximises the distance between the closest same-colour neighbours. Continental coverage.

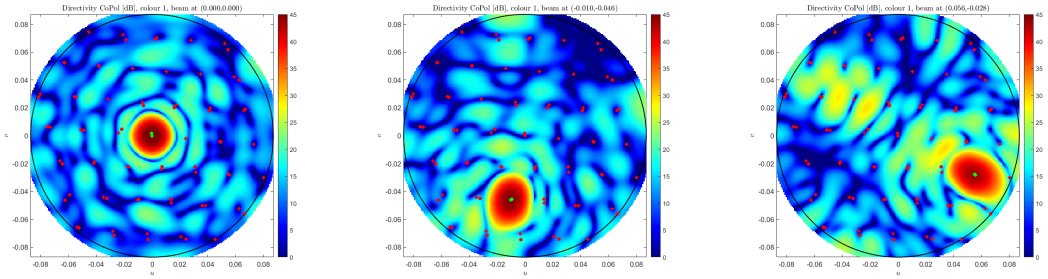

(a) Beam 1. (b) Beam 2. (c) Beam 3.

Figure 6: Plot of three different beams in colour 1. The green cross corresponds to the active beam's centre, while the green dot the corresponding user. The red crosses correspond to the remaining same colour's beam centres, while the red points the remaining users assigned to the same colour.

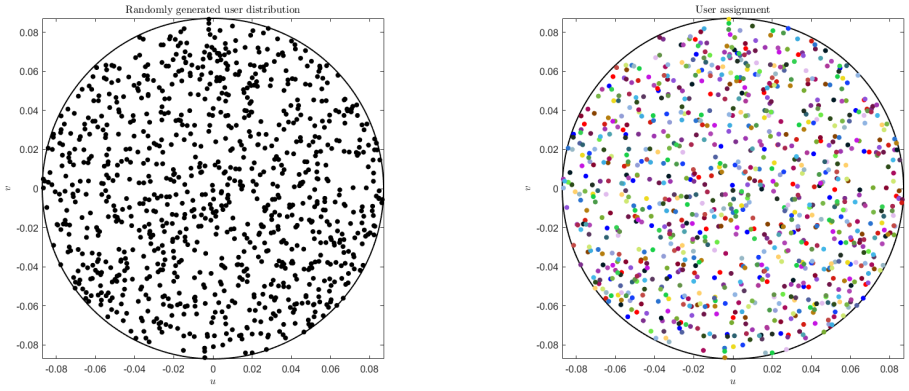

(a) Before RRM. (b) After RRM.

Figure 7: Randomly generated uniform user distribution before (a) and after (b) RRM.

resulting interference will be negligible compared to the receiver noise level. From Fig.6, we can also observe that the spacing between the same colour beams must be carefully selected based on the average beam beamwidth.

6 Extended Heuristic Radio Resource Management Algorithm

The RRM problem can be mathematically expressed as a colouring problem. In the framework of the project, each colour corresponds to one of the 41 sub-bands of 50MHz. The objective of RRM is to share the resources among the users in such way that interference is minimized. As a simplification, we assumed that users that are assigned to different colours do not interfere with each other (colour orthogonality). Fig.7b shows one example of the RRM outcome for the randomly generated uniform population in Fig.7a.

However, due to the enormous number of possible solutions and the non-convexity of the optimization problem, finding the solution that maximises the sum rate of the system is impossible. Henceforth, in [4] the authors have developed an heuristic algorithm to solve the RRM problem. In the framework of the project, the algorithm has been extended to FDM systems and maximises the SNIR rather than minimizing the interference. Due to space constraints the algorithm cannot be described in this document, but what follows is a short description. The algorithm assigns one user to one colour at every iteration. The user to be assigned at the n-th iteration can be chosen in different ways. One possibility is to select the user that would experience the worst SNIR if assigned to the wrong colour by considering the interference coming from all the already assigned users. Then, the assigned colour corresponds to the one that provides the largest SNIR.

Fig.8a, Fig.8b, and Fig.8c show the users assigned to colour 1, 2, and 3, respectively, by the extended H-RRM algorithm. These also correspond to the first three colours in Fig.7b. What is evident from these figures is that the extended H-RRM algorithm succeeded in assigning one user per beam. Furthermore, the distance between the users' location and the corresponding beam's centre is small. This ensures high SNIR values.

Finally, the performance of the system are evaluated considering different uniform and non uniform traffic distributions with a variable number of users. Fig.9 shows the cumulative distribution function (CDF) of the rate of the users in Fig.7a, corresponding to a randomly generated uniform population with 1000 users. The blue curve corresponds to the case where the FB-BFN beamforming weights are computed with MF precoding, while the red curve is the one obtained using MMSE precoding. The plot confirms the expected improvement due to the presence of the nulls when MMSE precoding is applied. In fact, almost 50% of the users achieve 180Mbps or more when MMSE precoding is used, against 145Mbps or more when MF precoding is used.

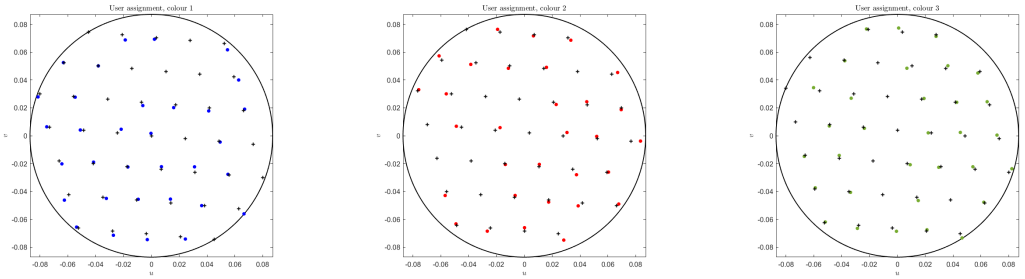

(a) Colour 1. (b) Colour 2. (c) Colour 3.

Figure 8: Plot of the colour assignment obtained with the extended H-RRM algorithm for the first three colours. The crosses represent the corresponding colour beam centres, while the dots correspond to the users assigned to the colour.

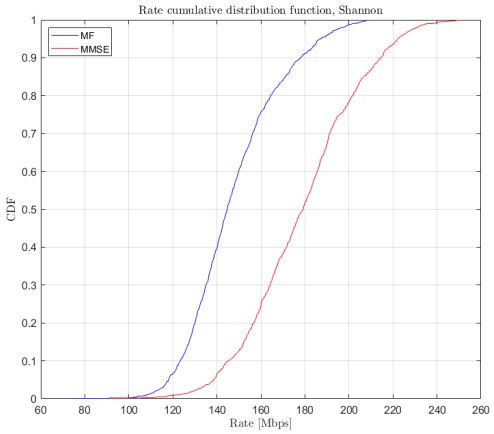

Figure 9: Plot of the cumulative distribution function of the rate of the user population in Fig.7a.

7 Conclusions

In the framework of this OSIP project, we developed a pragmatic AFR architecture suitable for broadband GEO communication satellites. Both the antenna and the payload have been studied and developed. The fully digital shaped AFR architecture has been optimize to operate in two different configurations, which correspond to two different defocusing distances of the feed array that can be adjusted on the fly. The shaping optimization guarantees a better distribution of the power across the feed array element, allowing the power amplifiers to operate more efficiently. A single antenna system has been optimised that guarantees high performance in different uniform and non uniform traffic scenarios. To provide high data rates while keeping the computational complexity limited, the DBFN is implemented as the cascade of a beam selection network and a FB-BFN. The FB-BFN beamforming weights are computed on Earth, transmitted to the satellite, which stores them. MMSE precoding based grids can be computed with each beam's centre corresponding to nulls of all the other beams. This solution, combined with the RRM algorithm, allows to achieve high SNIR values. Finally, an extended version of the H-RRM algorithm described in [4] has been developed. The simulation results confirmed the effectiveness of the proposed architecture, while maintaining a limited complexity of the payload.

References

[1] R. D. Gaudenzi, P. Angeletti, D. Petrolati, and E. Re, "Future technologies for very high throughput satellite systems," *International Journal of Satellite Communications and Networking*, vol. 38, pp. 141–161, 3 2020.

[2] C. Nicolas, V. Enjolras, P. Voisin, C. Boustie, and G. Jestin, "Thales alenia space 6th generation digital transparent processor (dtp6g) - a multi-mission, multi-mode versatile product at the heart of telecom solutions," *IET Conference Proceedings*, vol. 2022, pp. 25–32, 2022.

[3] P. Angeletti and R. D. Gaudenzi, "A pragmatic approach to massive mimo for broadband communication satellites," *IEEE Access*, vol. 8, pp. 132 212–132 236, 2020.

[4] ——, "Heuristic radio resource management for massive mimo in satellite broadband communication networks," *IEEE Access*, vol. 9, pp. 147 164–147 190, 2021.

[5] A. Baldominos, S. Mercader-Pellicer, G. Goussetis, A. Mengali, and N. J. Fonseca, "Heras: A modular matlab tool using physical optics for the analysis of reflector antennas," *Sensors 2023, Vol. 23, Page 1425*, vol. 23, p. 1425, 1 2023.

[6] V. Lakshminarayanan and A. Fleck, "Zernike polynomials: a guide," *Journal of Modern Optics*, vol. 58, pp. 545–561, 4 2011. [Online]. Available: https://www.tandfonline.com/doi/abs/10.1080/09500340.2011.554896

[7] D. A. Vieira, R. H. Takahashi, and R. R. Saldanha, "Multicriteria optimization with a multiobjective golden section line search," *Mathematical Programming*, vol. 131, pp. 131–161, 2 2012. [Online]. Available: https://link.springer.com/article/10.1007/s10107-010-0347-9

[8] F. Lisi, J. Maurin, H. Legay, P. Angeletti, and G. Goussetis, "Aperture distribution method for array-fed reflectors: a system level performance case study," *18th European Conference on Antennas and Propagation, EuCAP 2024*, 3 2024, (accepted).